More Than Another Halochromic Polymer: Thiazole-based Conjugated Polymer Transistors for Acid-sensing Applications

Zhibo Yuan[†], Qianyi Qu[‡], Kyle Hamrock[‡], Carolyn Buckley[†], Guoyan Zhang[‡], Elsa Reichmanis[†‡§*]

[†]*School of Chemistry and Biochemistry, Georgia Institute of Technology, 901 Atlantic Dr., Atlanta, GA 30309, United States*

[‡]*School of Chemical and Biomolecular Engineering, Georgia Institute of Technology, 311 Ferst Dr., Atlanta, GA 30332, United States*

[§]*School of Material Sciences and Engineering, Georgia Institute of Technology, 771 Ferst Dr., Atlanta, GA 30332, United States*

Keywords: conjugated polymers, thiazole, halochromism, organic thin-film transistor devices, sensors

*Author to whom correspondence should be addressed: elr420@lehigh.edu

Abstract

Stimuli-responsive π-conjugated materials present opportunities for chemical sensing, whereby through interaction with an analyte, the π-conjugated system undergoes a change in molecular geometry and/or electronic structure that can be detected as a change in either the optical or electrical characteristics. Here, a naphthalene diimide donor-acceptor conjugated polymer, poly(2,7-bis(2-decyltetradecyl)-4-methyl-9-(5'-methyl-[2,2'-bithiazol]-5-yl)benzo[lmn][3,8]-phenanthroline-1,3,6,8(2H,7H)-tetraone) (**PNDI2Tz**) is reported as an acid sensing material. Shifts in the UV-*vis* spectroscopic signature of **PNDI2Tz** in the presence of protic and Lewis Acids were investigated. Further, **PNDI2Tz**-based *n*-channel organic field-effect transistors (OFETs) were fabricated and shown to respond to the gas phase Lewis acid, boron trifluoride (BF_3), whereby the transistors reproducibly turn off in the presence of 60 ppm BF_3.

Introduction

Functional π-conjugated materials are beginning to emerge as attractive stimuli-responsive platforms for applications ranging from pressure sensitive devices to chemical sensors[1-11]. In the latter case, selective interaction between a target analyte (*i.e.* volatile chemicals, biological macromolecules, ions, particles) and a π-conjugated system effects changes in electronic structure and/or molecular geometry that impact the system's optical or electronic properties[3, 12, 13]. For example, π-conjugated compounds that undergo a change in either their absorbance or fluorescence spectrum upon interaction with ionic analytes containing iodide[14], cyanide[15], and ionic forms of mercury[14] and zinc,[16, 17] have been reported. In addition, π-conjugated materials are also known to interact with biological systems,[18], and in select cases exhibit halochromic effects upon changes in pH[19]. Polyaniline (PANI) is arguably one of the earliest π-conjugated polymers to be incorporated into a sensor platform.[21-23] PANI can exist in several forms, including the emeraldine base and emeraldine salt form which were shown to be effective for the reversible sensing of NH_3 and HCl using spectrophotometric analysis. In the presence of hydrazine, the salt is readily converted to the leucoemeraldine form, thus creating an avenue for the detection of this highly toxic, volatile compound.[23] More recently, interest has turned toward semiconducting molecule and polymer platforms for sensor applications because they enable the sensitive detection of analytes via an electronic device platform. For instance, Huang. et al. fabricated organic field effect transistors (OFETs) using copper or cobalt phthalocyanine blended with tris(pentafluorophenyl)borane as a receptor that was capable of selective sensing of NH_3, with a detection limit to 350 ppb v/v.[6] Mechanistically, NH_3 forms a complex with the substituted borane through B−N and hydrogen bonding interactions. Molecular organic semiconductors have also been reported to be effective for the detection of citric acid and a range of other organic acids that are common in biological systems.[20] Studies related to the direct detection of analytes by a polymer semiconductor have been less widely reported.

The examples provided above typically require incorporation of additional components to bind with the analyte, which results in an increase in system complexity. Semiconducting polymers, particularly donor-acceptor (D-A) semiconductors, present an interesting alternative, where several conjugated units that possess functionalities that could directly bind to a number of toxic species can be identified. Among the π-conjugated molecular architectures reported to date, thiazole-based materials are garnering increasing attention because the nitrogen-bearing moiety can be used to effectively manipulate frontier molecular orbital energies[24-27], and facilitate directed intermolecular interactions in solution[28, 29] and in the solid-state[30, 31]. For instance, thiazoles have been suggested as a promising building block for a new generation of electron transporting conjugated polymers for organic electronics applications, such as organic photovoltaics (OPV)[32-35], and organic field-effect transistors (OFET)[35-38]. Further, the nitrogen atom, integral to thiazole, imparts a level of basicity that may allow for acid-base interactions that are foundational for the design of halochromic materials. Mechanistically, the halochromic response of thiazole-based compounds is based on the activation of intramolecular charge transfer absorption that results from protonation and/or interaction with a Lewis acid. In general, π-conjugated structures with strong, built-in donor–acceptor interactions are expected to exhibit a more pronounced halochromic effect due to an enhanced ability to redistribute charge density and promote charge-transfer (CT) absorption.[19]

Here, we investigated the response of the thiazole-based donor-acceptor (D-A) conjugated polymer, poly(2,7-bis(2-decyltetradecyl)-4-methyl-9-(5'-methyl-[2,2'-bithiazol]-5-yl)benzo[lmn]-[3,8]-phenanthroline-1,3,6,8(2H,7H)-tetraone) (**PNDI2Tz**), to both protic and

Lewis acids. Studies explored **PNDI2Tz** response in the solution state and solid state (**Figure 1**), where pronounced halochromic behavior was observed. Furthermore, in the solid state, **PNDI2Tz** exhibited a change in electronic characteristics upon exposure to the representative Lewis acid, boron trifluoride (BF_3) when the polymer was incorporated as the active layer in organic field-effect transistor (OFET) devices. The results obtained here facilitated evaluation of the acid sensing mechanism and provide a platform for the future development of robust, low-cost and effective sensor technologies.

Experimental

Materials and Measurements

PNDI2Tz was synthesized and prepared according to literature procedures.[39, 40] Detailed characterization results are presented in the Supporting Information (S.I.). All reagents, solvents and acids were purchased from commercial sources, and were of reagent grade. Chloroform, dichloromethane, toluene, *p*-xylene, isopropanol, tetrahydrofuran (THF), dimethylformamide (DMF), chlorobenzene, 1,2-dichorobenzene (*o*-DCB), and 1,2,4-trichlorobenzene (TCB) were purchased as anhydrous grade solvents from Sigma-Aldrich. *N*-octadecyltrichlorosilane (OTS), was purchased from Gelest, Inc. Silica gel was purchased from Sorbent Technologies (Premium Rf™, porosity: 60Å; particle size: 40-75 μm).

All polymer thin films for UV-*vis* absorption characterization were prepared by spin-coating polymer solutions in *p*-xylene (5 mg/mL) or chloroform (5 mg/mL), onto pristine SiO_2 glass substrates and pre-treated glass coverslip substrates. Low concentration OTS solutions (0.1% v/v in toluene) were prepared in a N_2 filled glovebox. UV-ozone cleaned device substrates were transferred into a N_2 filled glovebox immediately after cleaning, and then submerged in the as prepared surface treatment solution overnight at room temperature. The passivated substrates were then bath sonicated in toluene for 30 min, followed by blow drying with compressed air (after passing through a bed of molecular sieves to remove water and oil).

For device studies, substrates were coated with the semiconductor ink (prepared by dissolution of 5-10 mg of polymer in *p*-xylene) using an in-house blade coater equipped with a glass blade and temperature-controlled heating stage. Blade coating speeds were programmed and precisely controlled by a DMX-UMD 23 controller from Arcus Technology. Blade height was controlled to be within a range of 45-55 μm, and blade angle was set to be 8° ± 1°. Heating during blade coating was achieved by embedded thermocouples with precise temperature control. For chloroform samples, the heating temperature was set at 45 °C; for *p*-xylene samples, the temperature was set at 100 °C.

UV-*vis* Measurements (halochromism). For solution UV-*vis* spectroscopy, **PNDI2Tz** stock solution in *p*-xylene was prepared at a concentration of 0.5 mg/mL, equivalent to a repeating-unit molar concentration of approximately 4.5×10^{-5} mol/L. **PNDI2Tz** used in this study had a number average molecular weight of 49.3 kD with a polydispersity index ($Đ$) of 3.33, as determined by gel permeation chromatography (GPC) relative to polystyrene standards using 1,2,4-trichlorobenzene as the eluent at a temperature of 135 °C. The as prepared *p*-xylene stock solution was heated to 100 °C in a N_2 filled glovebox for 30 min to disassemble polymer aggregates, and was subsequently passed through a 0.2 μm PTFE filter (VWR, part number 28145-499). **PNDI2Tz** stock solution (1.8 mL) was then transferred to a 1 cm × 1 cm quartz cuvette which was then sealed with a Teflon cap. Acid stock solutions in acetonitrile (MeCN; acid concentration of 1.02×10^{-3} M) were prepared in a similar fashion. A gas tight syringe was used to transfer a specified amount of diluted acid solution into the UV-*vis* cuvette that contained

PNDI2Tz stock solution. Between adding acid aliquots to the cuvette, the syringe was rinsed three times with MeCN, and then rinsed three times with the stock acid solution. The active species was confirmed to be H^+ by through addition of complementary NO_3^- (**Figure S1**). For thin-film UV-*vis* spectroscopy, **PNDI2Tz** in chloroform and/or *p*-xylene stock solution (4-6 mg/mL) were blade coated onto UV-ozone cleaned SiO_2 glass slides.

For experiments that exposed **PNDI2Tz** OFETs to BF_3, a custom apparatus was designed and constructed. The apparatus comprised a stainless steel base (interior W×L×H: 30cm×30cm×30cm), with plexiglass sides where epoxy glue was used as the sealant. The system was equipped with two gas inlets (BF_3 and N_2), and one gas outlet connected to a vial of triethylamine solution for neutralization of BF_3 (shown in S.I.). Prior to each experiment, the chamber was purged with N_2 for 3 min to ensure an inert anhydrous environment. Then, anhydrous $BF_3 \cdot OEt_2$ which was used as the source of BF_3 was introduced into the chamber. All waste BF_3 was neutralized with trimethylamine (TEA), and all measurements were performed in an exhaust hood with appropriate ventilation.

Results and Discussion

PNDI2Tz was synthesized and characterized as previously reported[41], and purified by Soxhlet extraction. The low-molecular-weight portions and residual catalyst impurities were removed by sequential dissolution in ethanol, acetone, and hexane. The chloroform extracts were concentrated and precipitated in methanol, and then the solids were collected as product.

Brønsted acid sensing. The **PNDI2Tz**-acid interaction was first explored in solution using a variety of acids including sulfuric acid (H_2SO_4), trifluoroacetic acid (TFA) and nitric acid (HNO_3) (UV-*vis* of **PNDI2Tz** upon addition of sulfuric acid and trifluoroacetic acid are presented in

Figures S2 and S3 in the supporting information). Upon addition of acid, **PNDI2Tz** solution changed color from pink to yellow within the first minute. HNO_3 was used for mechanistic studies since the monoprotic acid facilitated determination of H^+ equivalence. In addition, diluted nitric acid presented a safer alternative than trifluoroacetic acid. As visualized in **Video S1** in the Supporting Information, injection of 3M HNO_3 effected a rapid (within 5 s) color change in a process that was readily reversed upon addition of methanol (MeOH); and the cycle could be repeated over multiple times (**Figure 2**). Note that MeOH is a poor solvent for **PNDI2Tz** and thus addition of MeOH resulted in reduced solution transparency due to polymer aggregation.

The colorimetric process was then monitored via addition of stoichiometric quantities of HNO_3 in MeCN (1.02×10^{-3} M) to a solution of **PNDI2Tz** in *p*-xylene (1.8 mL, approx. 4.5×10^{-5} M). As presented in **Figure 3a**, after addition of 0.3 equivalents of nitric acid (relative to the repeat unit of **PNDI2Tz**), no further spectral changes were observed, suggesting a saturation threshold. Specifically, addition of the protic acid led to a decrease in the π-π^* absorbance at 540 nm (2.30 eV) with concomitant increase in absorbance at 450 nm (2.76 eV). The relative absorbance of these signature bands (A_{540}/A_{450}) was used to evaluate the sensitivity of **PNDI2Tz** toward HNO_3 (**Figure 3b**). Incremental addition of 0.025 *eq.* of the acid, resulted in apparent saturation of the system within 12 injections of acid, facilitating rapid sensing of H^+. The results demonstrated a linear relationship between the absorbance ratio (A_{540}/A_{450}) and H^+ equivalence (R^2=0.985). During acidification, the **PNDI2Tz** optical bandgap increased from 2.12 eV to 2.26 eV (pristine onset absorption at 584 nm, after acid onset absorption at 549 nm). In addition, an isosbestic point was apparent at ca. 485 nm (**Figure 3a**), indicating that the stoichiometry of the reaction remained unchanged and that no secondary reactions occurred during the considered time range. The results support the premise that **PNDI2Tz** is a weak Lewis base that forms a weak acid-base adduct with H^+. The active species is most likely H^+: addition of a complementary ion such as Na^+ or K^+ through addition of the corresponding nitrates in acetonitrile resulted in no observable spectral change (**Figure S1**). This hypothesis finds additional support from results reported by Yamamoto and co-workers, who demonstrated that trifluoroacetic acid can protonate the nitrogen in thiazole moieties, based on ^{15}N NMR spectroscopy results.[42, 43] It is noted that the acid detection limit for PNDI2Tz is 0.3 eq. This equivalence is the ratio of H^+ to the PNDI2Tz repeating unit.

Lewis acid sensing: Having established the ability of **PNDI2Tz** to interact with strong protic acids, the investigation was extended to explore the impact of exposure to neutral Lewis acid species. Specifically, BF_3 was selected as a representative example[44] given its ready availability, commercial significance and known environmental health and safety issues and relatively low LC_{50}.[45-48]. As stated in the AEGL book, the AEGL-3 can be treated as the LC_{50} for BF_3, which is at 436.22 ppm (1210 mg/m^3) for rats on 4-hour exposure.[49] In this study, fresh anhydrous $BF_3 \cdot OEt_2$ was used as the source of BF_3 to facilitate handling. The response of **PNDI2Tz** to the Lewis acid was evaluated in both xylene solution and solidified thin film state.

While solutions of **PNDI2Tz** underwent a color change upon exposure to $BF_3 \cdot OEt_2$, the ability to detect low levels of atmospheric BF_3 vapor presents a more relevant and challenging application. Thus, the response of **PNDI2Tz** thin-films to the presence of controlled amounts of BF_3 was investigated both spectroscopically and electronically. Initial studies focused on the spectroscopic/colorimetric response. Using a custom built, controlled atmosphere apparatus, **PNDI2Tz** coated glass slides were treated with BF_3. Upon injection of $BF_3 \cdot OEt_2$ (20 μL, 0.16 mmol BF_3, 240 ppm) into the chamber, the initially pink **PNDI2Tz** thin film slowly changed color to yellow in a reversible process, whereby the sample regained its original pink hue within

5 min under ambient conditions (**Figure 4**). The spontaneous recovery process was monitored using UV-*vis* spectroscopy: the intensity of the π-π* **PNDI2Tz** absorption band centered at 543 nm (2.28 eV) increased, while that at 455 nm (2.73 eV) decreased, with an isosbestic point at 490 nm (2.53 eV) (**Figure 3a**). In addition, a shoulder observed at 387 nm (3.20 eV) in the BF_3 treated sample decreased in intensity, and was not longer apparent after 240 s. The observed spectroscopic changes were reversible, and mirrored the behavior of **PNDI2Tz** solutions upon exposure to protic acids, *vide supra*. Similar to the solution results, the **PNDI2Tz** optical bandgap increased upon exposure to acid, though in the case of the solidified film, the gap changed from 2.04 eV to 2.16 eV (pristine **PNDI2Tz** thin-film onset absorption at 607 nm, after BF_3 exposure onset absorption at 575 nm) (**Figure 5**).

Given the clear colorimetric response of **PNDI2Tz** thin-films, the macroscale electronic response of the electron transport conjugated polymer was investigated. **PNDI2Tz** was incorporated as the active layer into bottom gate bottom contact organic field effect transistors (experimental details associated with OFET fabrication are provided in the Supporting Information) and device response to BF_3 exposure was recorded. The device was first turned on, sweeping the gate with voltage from -25 V to 80 V. Once stable performance was achieved, 5 μL $BF_3 \cdot OEt_2$ (equivalent BF_3 concentration of 60 ppm) was introduced into the apparatus (**Figure S4**). In the presence of BF_3, the transistor turned off: the source-drain current (I_{sd}) decreased from approximately 10^{-4} A to a current in the range of 10^{-8}~10^{-10} A, representing a 4~6 order of magnitude change (**Figure 6**). The observed response was reversible upon exposure of the device to vacuum (−30 mmHg) for 3 min followed by purging with pure N_2. **PNDI2Tz** OFETs regained their transistor characteristics, exhibiting similar I_{sd} to untreated samples. Further, the impact of cycling the devices was evaluated over 50 cycles by monitoring the I_{sd} and threshold voltage and calculating semiconducting polymer mobility for each run (**Figure S5)**. I_{sd} gradually decreased after 10 cycles but remained above 20 μA, while threshold voltage (V_{th}) increased from -1 V to -4 V. OFET mobility decreased only slightly. Overall, the results suggest that **PNDI2Tz**-based OFET sensors are highly stable and robust. Results presented in **Figure S6** illustrate the OFET I_{sd} response during the first 6 min after introduction of the analyte. Upon exposure to anhydrous $BF_3 \cdot OEt_2$, OFET performance degraded significantly, exhibiting essentially no transistor response. No change in source-drain current was observed in control experiments using anhydrous ethyl ether, confirming that the active species was BF_3.

Acid Sensing Mechanism: While thiazoles have been only recently introduced as molecular entities of interest for semiconducting polymer applications, they have long been used as ligands in biologically active materials such as bleomycin, a medication used to treat cancer.[50, 51] Further, the ability of thiazole to form chelates or coordination compounds with metal ions has been studied extensively.[42, 52-55] Thus, from a mechanistic perspective, the response of **PNDI2Tz** to acids may derive from weak interactions between acidic species and the nitrogen lone pair residing on the bithiazole moiety of **PNDI2Tz** (**Figure 7**). For instance, in the case of BF_3, the Lewis Acid may interact weakly with the conjugated polymer repeating unit to form a Lewis acid-Lewis base (LA-LB) adduct. Further, given that the response to H^+ saturates after addition of only 0.3 acid equivalents and that an isosbestic point is observed, the sensing mechanism is unlikely to proceed via stepwise addition of acid to each thiazole unit. In addition, recall that the **PNDI2Tz** optical bandgap increased in the presence of acid, pointing to a decrease in the conjugation length; suggesting that upon adduct formation, the torsion angle between the thiazole rings increases, leading to an increased HOMO-LUMO energy gap. The apparent change in molecular geometry, a.k.a., twist in the bithiazole structure from nominally planar to non-planar[41], likely hinders binding with a second acidic species. Computational and resonance Raman spectroscopic studies could further elucidate the mechanism associated with **PNDI2Tz** response to acidic species.

Summary

In summary, the response of a thiazole-based conjugated polymer, **PNDI2Tz** to both protic and Lewis acids was investigated. In addition to presenting a colorimetric response in solution and solid films, **PNDI2Tz**-based *n*-channel OFETs were fabricated and device electronic response against the vapor-phase Lewis acid, BF_3 was evaluated. **PNDI2Tz** exhibited strong response to ppm levels of BF_3 through formation of a Lewis acid-base adduct; which led to a significant reduction in charge transport performance, which is believed to derive from interactions between the bithiazole nitrogen lone pair and the acidic species. **PNDI2Tz** and its analogs possess significant potential for new, low-power OFET-based acid sensor designs. Further, the results suggest the ability to tune the molecular structure and geometry of donor-acceptor (and/or acceptor-acceptor) conjugated polymers to pave new directions for the design and development of advanced and ubiquitous sensors for environmental monitoring.

Author Information

Corresponding author:
Elsa Reichmanis: elr420@lehigh.edu

ORCID
Elsa Reichmanis: 0000-0002-8205-8016

Current Address:
Elsa Reichmanis, Department of Chemical and Biomolecular Engineering, Lehigh University, Bethlehem, PA 18015
Zhibo Yuan, Applied Materials, 3050 Bowers Avenue, Santa Clara, CA 95054

The authors declare no competing financial interest

Acknowledgements:
The authors would like to acknowledge support from the National Science Foundation Grant No. 1809495: Interplay of Molecular Structure and Solution Behavior in High Performance Conjugated Polymers, the Georgia Institute of Technology, and the Pete Silas Chair funds for support. C.B. also acknowledges NSF IGERT NESAC Traineeship support: NSF Grant No. 1069138: Nanostructured Materials for Energy Storage and Conversion. This work was performed in part at the Georgia Tech Institute for Electronics and Nanotechnology, a member of the National Nanotechnology Coordinated Infrastructure, which is supported by the National Science Foundation (ECCS-1542174).

Supporting Information Available:
Statement on boron trifluoride LD/LC_{50} and OSHA standards; description of methodology of thin film and device fabrication; experimental description of complementary ion addition in PNDI2Tz solution with associated spectroscopic data; image of PNDI2Tz OFET-based BF_3 sensor in custom-built apparatus to evaluate response to BF_3; transistor data depicting sensor stability.

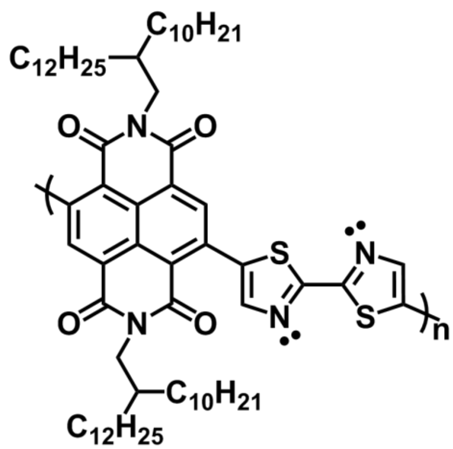

Figure 1. Chemical structure of PNDI2Tz showing nitrogen atom lone pairs.

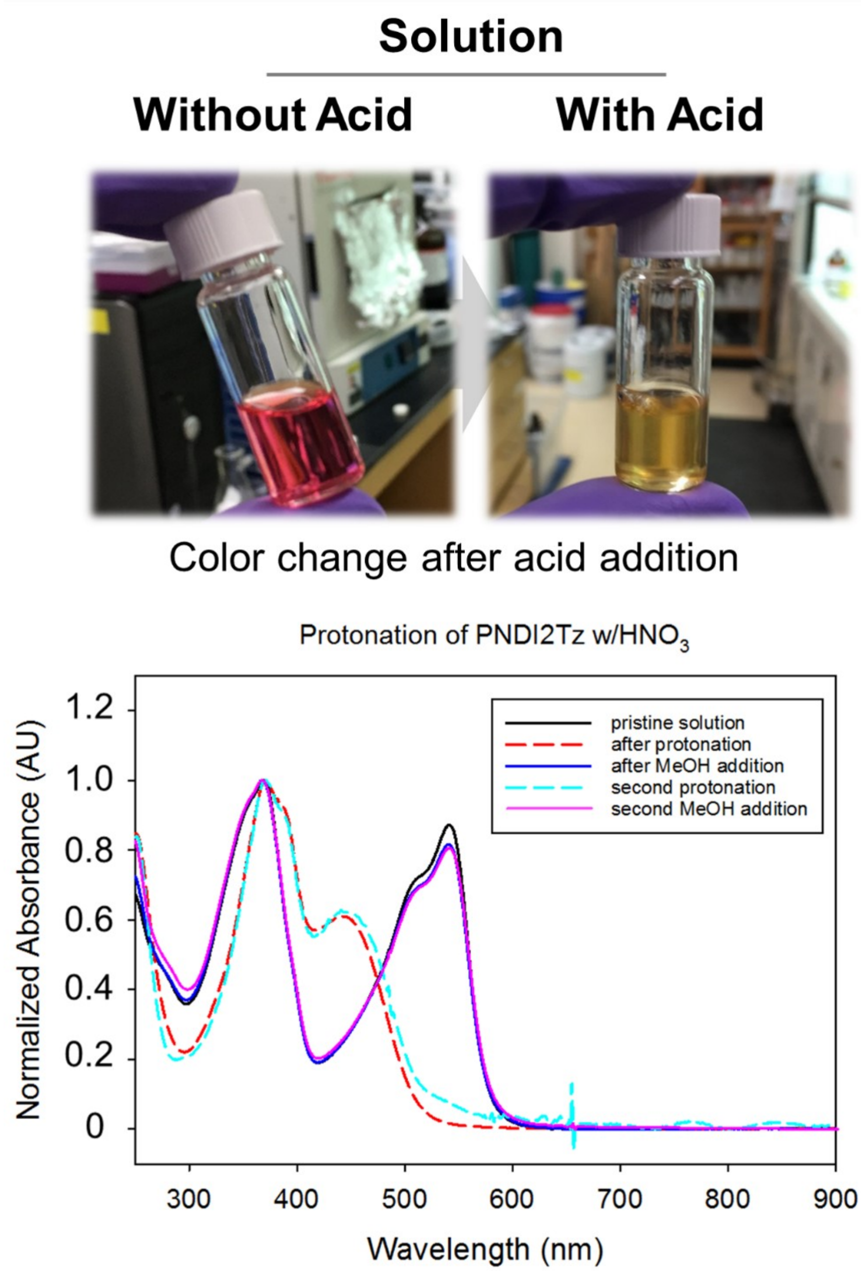

Figure 2. (top) PNDI2Tz halochromic effect in solution with HNO_3 addition; (bottom) UV-vis spectra of PNDI2Tz solution during acidification cycles.

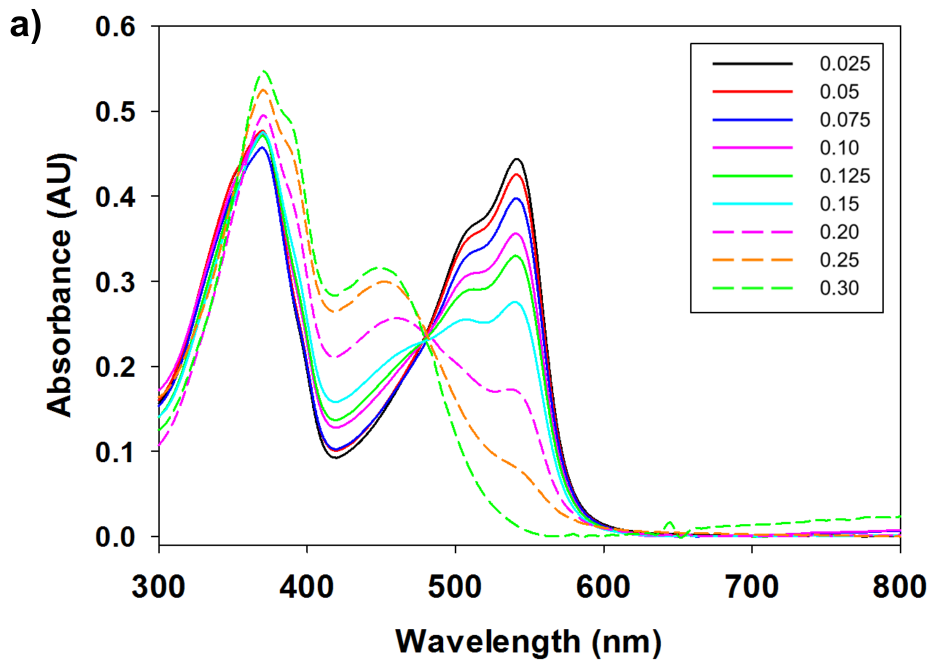

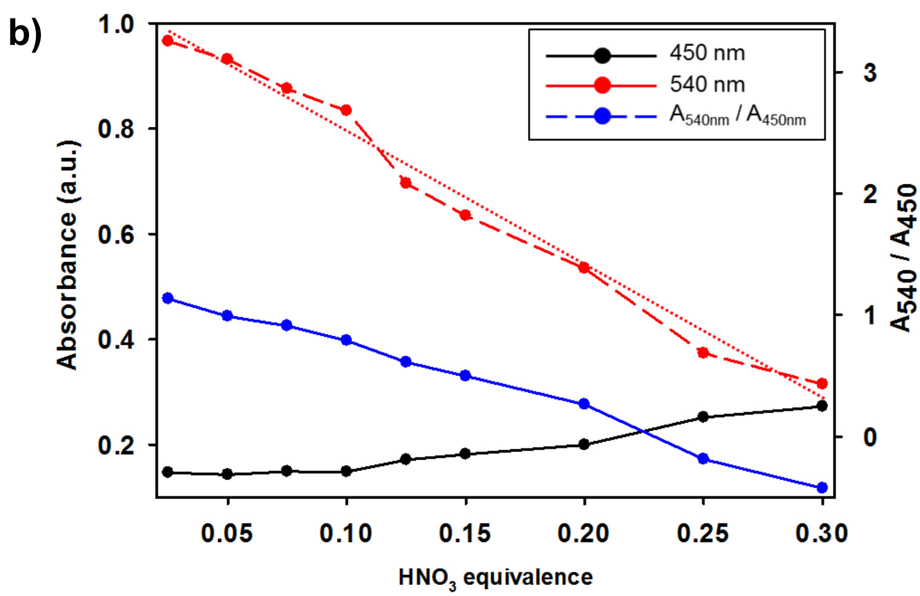

Figure 3. a) Stoichiometric addition of HNO_3 to PNDI2Tz solution with HNO_3 molar equivalences. b) Relative absorbance (A_{540}/A_{450}) with respect to different HNO_3 molar equivalences.

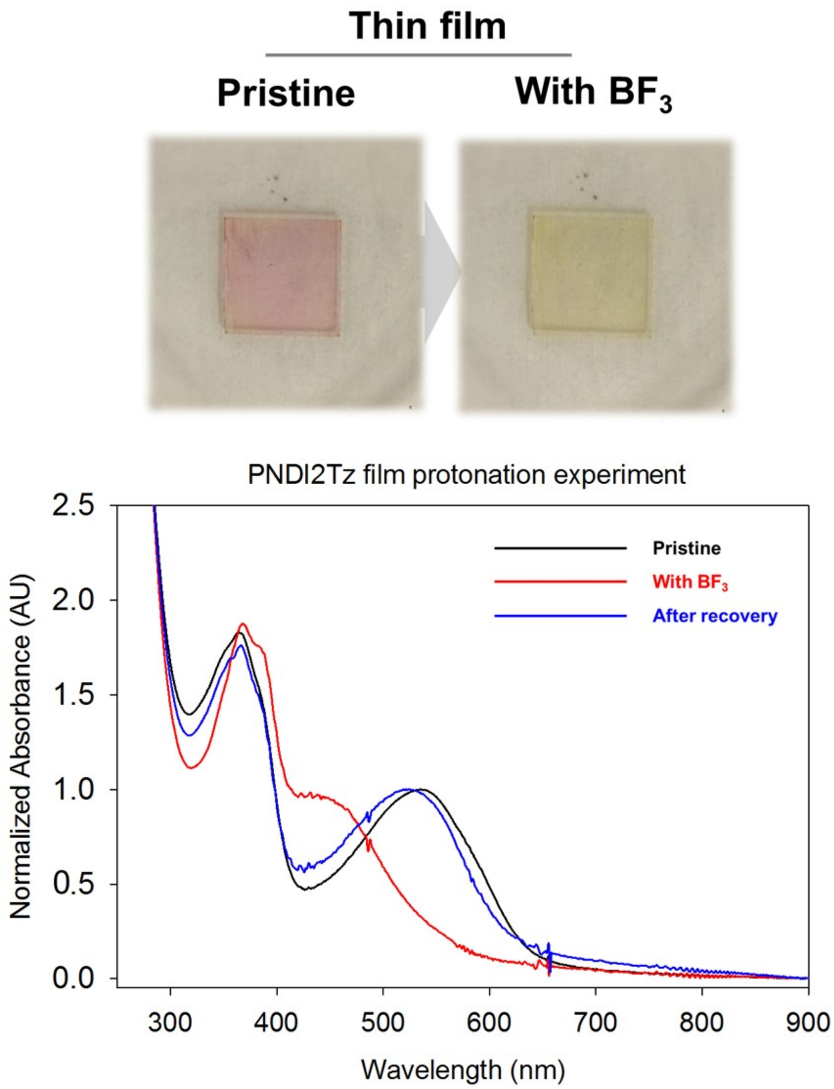

Figure 4. (top) PNDI2Tz solid state halochromic effect upon exposure to BF_3; (bottom) UV-vis spectra of PNDI2Tz thin film during BF_3 cycles.

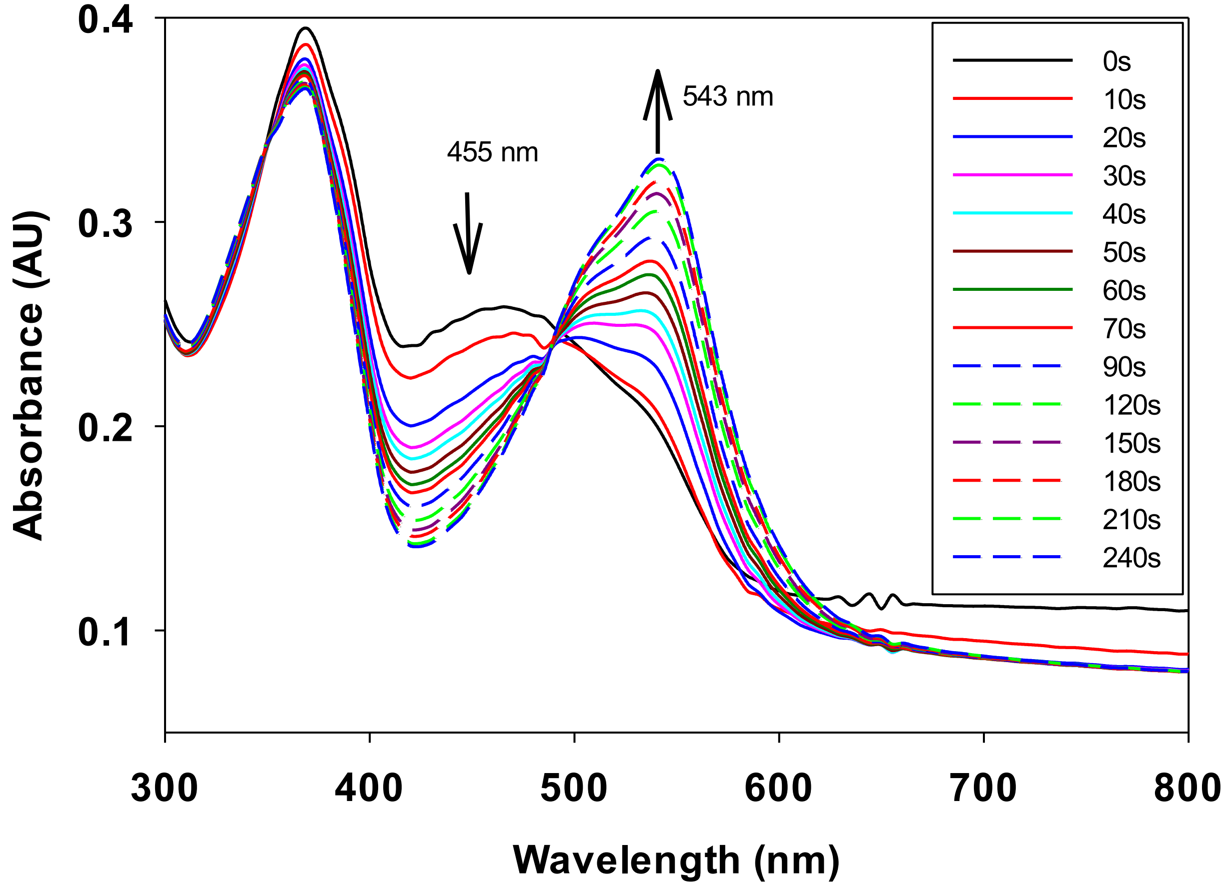

Figure 5. Overlaid UV-*vis* spectra of PNDI2Tz recovery process after BF_3 exposure.

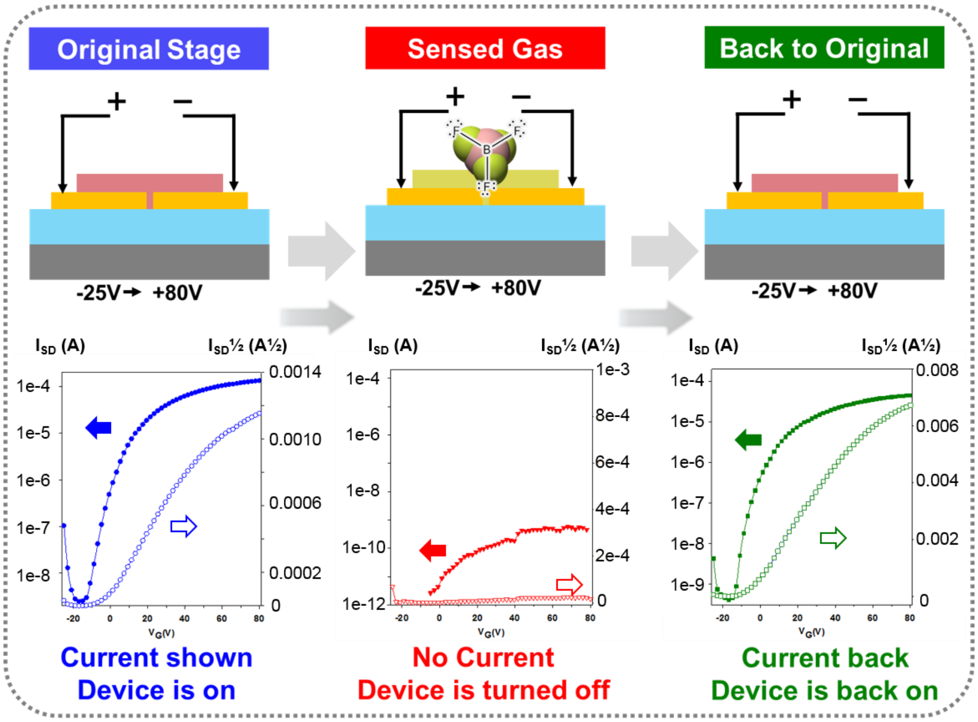

	Original Stage	Sensed Gas	Back-to-original
On-Current (I_{ON})	134 μA (± 21 μA)	Lower than 1 nA	98 μA (± 17 μA)
Threshold Voltage (V_{th})	-1.4 V (± 0.5V)	Not measurable	-2.8 V (± 1.7 V)
Mobility (μ_e^{FET})	0.043 cm^2/Vs (± 0.003 cm^2/Vs)	No mobility measured	0.035 cm^2/Vs (± 0.008 cm^2/Vs)

Figure 6. Demonstration of PNDI2Tz OFET-based BF3 sensor with transfer curves

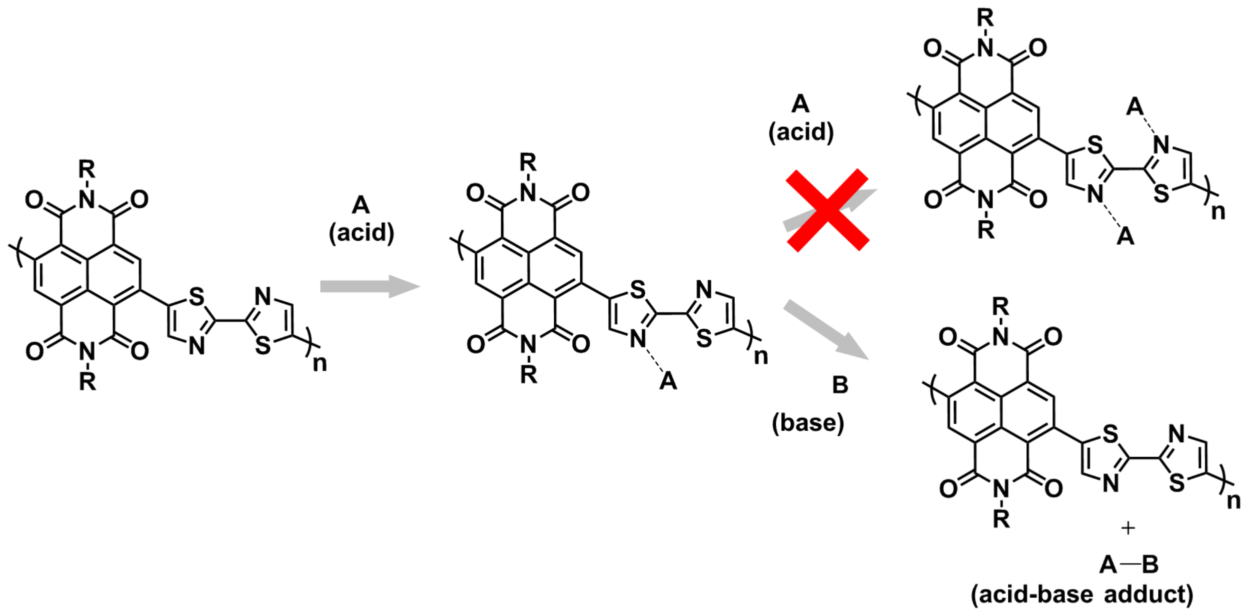

Figure 7. Proposed mechanism of PNDI2Tz interaction with acids

References:

1. Someya, T.; Katz, H. E.; Gelperin, A.; Lovinger, A. J.; Dodabalapur, A. Vapor sensing with α,ω-dihexylquarterthiophene field-effect transistors: The role of grain boundaries. *Appl. Phys. Lett.* **2002,** 81 (16), 3079-3081.
2. Crone, B. K.; Dodabalapur, A.; Sarpeshkar, R.; Gelperin, A.; Katz, H. E.; Bao, Z. Organic oscillator and adaptive amplifier circuits for chemical vapor sensing. *J. Appl. Phys.* **2002,** 91 (12), 10140-10146.
3. Crone, B.; Dodabalapur, A.; Gelperin, A.; Torsi, L.; Katz, H. E.; Lovinger, A. J.; Bao, Z. Electronic sensing of vapors with organic transistors. *Appl. Phys. Lett.* **2001,** 78 (15), 2229-2231.
4. Someya, T.; Dodabalapur, A.; Huang, J.; See, K. C.; Katz, H. E. Chemical and Physical Sensing by Organic Field-Effect Transistors and Related Devices. *Adv. Mater.* **2010,** 22 (34), 3799-3811.
5. McQuade, D. T.; Pullen, A. E.; Swager, T. M. Conjugated Polymer-Based Chemical Sensors. *Chem. Rev.* **2000,** 100 (7), 2537-2574.
6. Huang, W.; Besar, K.; LeCover, R.; Rule, A. M.; Breysse, P. N.; Katz, H. E. Highly Sensitive NH3 Detection Based on Organic Field-Effect Transistors with Tris(pentafluorophenyl)borane as Receptor. *J. Am. Chem. Soc.* **2012,** 134 (36), 14650-14653.
7. Torsi, L.; Farinola, G. M.; Marinelli, F.; Tanese, M. C.; Omar, O. H.; Valli, L.; Babudri, F.; Palmisano, F.; Zambonin, P. G.; Naso, F. A sensitivity-enhanced field-effect chiral sensor. *Nat. Mater.* **2008,** 7, 412.
8. Torsi, L.; Magliulo, M.; Manoli, K.; Palazzo, G. Organic field-effect transistor sensors: a tutorial review. *Chem. Soc. Rev.* **2013,** 42 (22), 8612-8628.
9. Kanda, M.; Puggal, S.; Dhall, N.; Sharma, A. Recent Developments in the Fabrication, Characterization, and Properties Enhancement of Polymer Nanocomposites: A Critical Review. *Materials Today: Proceedings* **2018,** 5 (14, Part 2), 28243-28252.
10. Khim, D.; Ryu, G.-S.; Park, W.-T.; Kim, H.; Lee, M.; Noh, Y.-Y. Precisely Controlled Ultrathin Conjugated Polymer Films for Large Area Transparent Transistors and Highly Sensitive Chemical Sensors. *Adv. Mater.* **2016,** 28 (14), 2752-2759.
11. Yang, Y.; Liu, Z.; Chen, L.; Yao, J.; Lin, G.; Zhang, X.; Zhang, G.; Zhang, D. Conjugated Semiconducting Polymer with Thymine Groups in the Side Chains: Charge Mobility Enhancement and Application for Selective Field-Effect Transistor Sensors toward CO and H2S. *Chem. Mater.* **2019,** 31 (5), 1800-1807.
12. Torsi, L.; Dodabalapur, A. Organic Thin-Film Transistors as Plastic Analytical Sensors. *Anal. Chem.* **2005,** 77 (19), 380 A-387 A.
13. Torsi, L.; Dodabalapur, A.; Sabbatini, L.; Zambonin, P. G. Multi-parameter gas sensors based on organic thin-film-transistors. *Sensors and Actuators B: Chemical* **2000,** 67 (3), 312-316.
14. Hussain, S.; De, S.; Iyer, P. K. Thiazole-Containing Conjugated Polymer as a Visual and Fluorometric Sensor for Iodide and Mercury. *ACS Appl. Mater. Interfaces* **2013,** 5 (6), 2234-2240.
15. Son, J. H.; Jang, G.; Lee, T. S. Synthesis of water-soluble, fluorescent, conjugated polybenzodiazaborole for detection of cyanide anion in water. *Polymer* **2013,** 54 (14), 3542-3547.
16. Helal, A.; Kim, H.-S. Thiazole-based chemosensor: synthesis and ratiometric fluorescence sensing of zinc. *Tetrahedron Lett.* **2009,** 50 (39), 5510-5515.
17. Helal, A.; Kim, S. H.; Kim, H.-S. Thiazole sulfonamide based ratiometric fluorescent chemosensor with a large spectral shift for zinc sensing. *Tetrahedron* **2010,** 66 (52), 9925-9932.

18. Hanafi-Bagby, D.; Piunno, P. A. E.; Wust, C. C.; Krull, U. J. Concentration dependence of a thiazole orange derivative that is used to determine nucleic acid hybridization by an optical biosensor. *Anal. Chim. Acta* **2000,** 411 (1), 19-30.
19. Black, H. T.; Pelse, I.; Wolfe, R. M. W.; Reynolds, J. R. Halochromism and protonation-induced assembly of a benzo[g]indolo[2,3-b]quinoxaline derivative. *Chem. Commun. (Cambridge, U. K.)* **2016,** 52 (87), 12877-12880.
20. Furusawa, H.; Ichimura, Y.; Harada, S.; Uematsu, M.; Xue, S.; Nagamine, K.; Tokito, S. Electric Charge Detection of Sparse Organic Acid Molecules Using an Organic Field-Effect Transistor (OFET)-Based Sensor. *Bull. Chem. Soc. Jpn.* **2018,** 91 (7), 1020-1025.
21. Huang, J.; Virji, S.; Weiller, B. H.; Kaner, R. B. Polyaniline Nanofibers: Facile Synthesis and Chemical Sensors. *J. Am. Chem. Soc.* **2003,** 125 (2), 314-315.
22. Nicolas-Debarnot, D.; Poncin-Epaillard, F. Polyaniline as a new sensitive layer for gas sensors. *Anal. Chim. Acta* **2003,** 475 (1), 1-15.
23. Virji, S.; Huang, J.; Kaner, R. B.; Weiller, B. H. Polyaniline Nanofiber Gas Sensors: Examination of Response Mechanisms. *Nano Lett.* **2004,** 4 (3), 491-496.
24. Takimiya, K.; Osaka, I.; Nakano, M. π-Building Blocks for Organic Electronics: Revaluation of “Inductive” and “Resonance” Effects of π-Electron Deficient Units. *Chem. Mater.* **2014,** 26 (1), 587-593.
25. Zaborova, E.; Chávez, P.; Bechara, R.; Lévêque, P.; Heiser, T.; Méry, S.; Leclerc, N. Thiazole as a weak electron-donor unit to lower the frontier orbital energy levels of donor–acceptor alternating conjugated materials. *Chem. Commun. (Cambridge, U. K.)* **2013,** 49 (85), 9938-9940.
26. Guo, X.; Quinn, J.; Chen, Z.; Usta, H.; Zheng, Y.; Xia, Y.; Hennek, J. W.; Ortiz, R. P.; Marks, T. J.; Facchetti, A. Dialkoxybithiazole: A New Building Block for Head-to-Head Polymer Semiconductors. *J. Am. Chem. Soc.* **2013,** 135 (5), 1986-1996.
27. Zhou, X.; Chen, P.; Koh, C. W.; Chen, S.; Yu, J.; Zhang, X.; Tang, Y.; Bianchi, L.; Guo, H.; Woo, H. Y.; Guo, X. Polymer semiconductors incorporating head-to-head linked 4-alkoxy-5-(3-alkylthiophen-2-yl)thiazole. *RSC Advances* **2018,** 8 (62), 35724-35734.
28. Blight, B. A.; Hunter, C. A.; Leigh, D. A.; McNab, H.; Thomson, P. I. T. An AAAA–DDDD quadruple hydrogen-bond array. *Nature Chem.* **2011,** 3, 244.
29. Schmuck, C.; Wienand, W. Self-Complementary Quadruple Hydrogen-Bonding Motifs as a Functional Principle: From Dimeric Supramolecules to Supramolecular Polymers. *Angewandte Chemie International Edition* **2001,** 40 (23), 4363-4369.
30. Luo, X.-Z.; Jia, X.-J.; Deng, J.-H.; Zhong, J.-L.; Liu, H.-J.; Wang, K.-J.; Zhong, D.-C. A Microporous Hydrogen-Bonded Organic Framework: Exceptional Stability and Highly Selective Adsorption of Gas and Liquid. *J. Am. Chem. Soc.* **2013,** 135 (32), 11684-11687.
31. Black, H. T.; Perepichka, D. F. Crystal Engineering of Dual Channel p/n Organic Semiconductors by Complementary Hydrogen Bonding. *Angewandte Chemie International Edition* **2014,** 53 (8), 2138-2142.
32. Li, W.; Roelofs, W. S. C.; Turbiez, M.; Wienk, M. M.; Janssen, R. A. J. Polymer Solar Cells with Diketopyrrolopyrrole Conjugated Polymers as the Electron Donor and Electron Acceptor. *Adv. Mater.* **2014,** 26 (20), 3304-3309.
33. Hendriks, K. H.; Li, W.; Heintges, G. H. L.; van Pruissen, G. W. P.; Wienk, M. M.; Janssen, R. A. J. Homocoupling Defects in Diketopyrrolopyrrole-Based Copolymers and Their Effect on Photovoltaic Performance. *J. Am. Chem. Soc.* **2014,** 136 (31), 11128-11133.

34. Bulut, I.; Chávez, P.; Mirloup, A.; Huaulmé, Q.; Hébraud, A.; Heinrich, B.; Fall, S.; Méry, S.; Ziessel, R.; Heiser, T.; Lévêque, P.; Leclerc, N. Thiazole-based scaffolding for high performance solar cells. *J. Mater. Chem. C.* **2016,** 4 (19), 4296-4303.
35. Lin, Y.; Fan, H.; Li, Y.; Zhan, X. Thiazole-Based Organic Semiconductors for Organic Electronics. *Adv. Mater.* **2012,** 24 (23), 3087-3106.
36. Fu, B.; Wang, C.-Y.; Rose, B. D.; Jiang, Y.; Chang, M.; Chu, P.-H.; Yuan, Z.; Fuentes-Hernandez, C.; Kippelen, B.; Brédas, J.-L.; Collard, D. M.; Reichmanis, E. Molecular Engineering of Nonhalogenated Solution-Processable Bithiazole-Based Electron-Transport Polymeric Semiconductors. *Chem. Mater.* **2015,** 27 (8), 2928-2937.
37. Yuan, Z. B.; Fu, B. Y.; Thomas, S.; Zhang, S. Y.; DeLuca, G.; Chang, R.; Lopez, L.; Fares, C.; Zhang, G. Y.; Bredas, J. L.; Reichmanis, E. Unipolar Electron Transport Polymers: A Thiazole Based All-Electron Acceptor Approach. *Chem. Mater.* **2016,** 28 (17), 6045-6049.
38. Shi, Y.; Guo, H.; Qin, M.; Zhao, J.; Wang, Y.; Wang, H.; Wang, Y.; Facchetti, A.; Lu, X.; Guo, X. Thiazole Imide-Based All-Acceptor Homopolymer: Achieving High-Performance Unipolar Electron Transport in Organic Thin-Film Transistors. *Adv. Mater.* **2018,** 30 (10), 1705745.
39. Guo, X. G.; Kim, F. S.; Seger, M. J.; Jenekhe, S. A.; Watson, M. D. Naphthalene Diimide-Based Polymer Semiconductors: Synthesis, Structure-Property Correlations, and n-Channel and Ambipolar Field-Effect Transistors. *Chem. Mater.* **2012,** 24 (8), 1434-1442.
40. Guo, X.; Watson, M. D. Conjugated polymers from naphthalene bisimide. *Org. Lett.* **2008,** 10 (23), 5333-6.
41. Yuan, Z.; Buckley, C.; Thomas, S.; Zhang, G.; Bargigia, I.; Wang, G.; Fu, B.; Silva, C.; Brédas, J.-L.; Reichmanis, E. A Thiazole–Naphthalene Diimide Based n-Channel Donor–Acceptor Conjugated Polymer. *Macromolecules* **2018,** 51 (18), 7320-7328.
42. Yamamoto, T.; Suganuma, H.; Maruyama, T.; Inoue, T.; Muramatsu, Y.; Arai, M.; Komarudin, D.; Ooba, N.; Tomaru, S.; Sasaki, S.; Kubota, K. π-Conjugated and Light Emitting Poly(4,4‘-dialkyl-2,2‘-bithiazole-5,5‘-diyl)s and Their Analogues Comprised of Electron-Accepting Five-Membered Rings. Preparation, Regioregular Structure, Face-to-Face Stacking, and Electrochemical and Optical Properties. *Chem. Mater.* **1997,** 9 (5), 1217-1225.
43. Wheelhouse, R. T.; Shi, D.-F.; Wilman, D. E. V.; Stevens, M. F. G. Antitumour benzothiazoles. Part 4. An NMR study of the sites of protonation of 2-(4-aminophenyl)benzothiazoles. *Journal of the Chemical Society, Perkin Transactions 2* **1996,** (7), 1271-1274.
44. Findlater, M.; Swisher, N. S.; White, P. S. Synthesis and Structure of Boron–Bithiazole Complexes. *Eur. J. Inorg. Chem.* **2010,** 2010 (34), 5379-5382.
45. The National Institute for Occupational Safety and Health (NIOSH), Boron trifluoride, Immediately Dangerous to Life or Health Concentrations (IDLH). (Publish year **1994**), https://www.cdc.gov/niosh/idlh/7637072.html (Accessed on October 27, **2019**).
46. LaDou, J. Potential occupational health hazards in the microelectronics industry. *Scandinavian Journal of Work, Environment & Health* **1983,** 9 (1), 42-46.
47. Chelton, C. F.; Glowatz, M.; Mosovsky, J. A. Chemical hazards in the semiconductor industry. *IEEE Transactions on Education* **1991,** 34 (3), 269-288.
48. Praxair, Safety Data Sheet P-4567: Boron trifluoride (CAS No. 7637-07-2). (Publish year **1979**), https://www.praxair.com/-/media/corporate/praxairus/documents/sds/boron-trifluoride-bf3-safety-data-sheet-sds-p4567.pdf?la=en&rev=4f634f1ebf5a4a5694b9203f7d2593dd (Accessed on October 27, **2019**).

49. Levels, C. o. A. E. G.; Toxicology, C. o.; Toxicology, B. o. E. S. a.; Studies, D. o. E. a. L.; National Academies of Sciences, E., and Medicine., *Acute Exposure Guideline Levels for Selected Airborne Chemicals*. National Academies Press (US): Washington (DC), 2016; Vol. 20.
50. Kane, S. A.; Natrajan, A.; Hecht, S. M. On the role of the bithiazole moiety in sequence-selective DNA cleavage by Fe.bleomycin. *J. Biol. Chem.* **1994,** 269 (14), 10899-10904.
51. Povirk, L. F.; Hogan, M.; Dattagupta, N. Binding of bleomycin to DNA: intercalation of the bithiazole rings. *Biochemistry* **1979,** 18 (1), 96-101.
52. Sugiura, Y. Monomeric cobalt(II)-oxygen adducts of bleomycin antibiotics in aqueous solution. A new ligand type for oxygen binding and effect of axial Lewis base. *J. Am. Chem. Soc.* **1980,** 102 (16), 5216-5221.
53. Lehmann, T. E. Molecular modeling of the three-dimensional structure of Fe(II)-bleomycin: are the Co(II) and Fe(II) adducts isostructural? *JBIC Journal of Biological Inorganic Chemistry* **2002,** 7 (3), 305-312.
54. Mahjoub, A.; Morsali, A. Hg(II), Tl(III), Cu(I), and Pd(II) Complexes with 2,2'-Diphenyl-4,4'-Bithiazole (DPBTZ), Syntheses and X-Ray Crystal Structure of [Hg(DPBTZ)(SCN)2]. *J. Coord. Chem.* **2003,** 56 (9), 779-785.
55. Shahbazi-Raz, F.; Notash, B.; Amani, V.; Safari, N. 4,4′ -Dimethyl-2,2′ -bithiazole: Potent co-former in coordination compounds. *Polyhedron* **2016,** 119, 227-237.

Corrected reference 49: National Research Council 2012. Acute Exposure Guideline Levels for Selected Airborne Chemicals: Volume 13. Pages 13-59. Washington, DC: The National Academies Press. https://doi.org/10.17226/15852

National Academies of Sciences, Engineering, and Medicine. 2016. *Acute Exposure Guideline Levels for Selected Airborne Chemicals: Volume 20*. Washington, DC: The National Academies Press. https://doi.org/10.17226/23634

Table of Contents Graphic (TOC):